

Anomalous High-Energy Second Plateau in High Harmonic Generation from Fullerenes

Km Akanksha Dubey* and Ofer Neufeld†

Technion- Israel Institute of Technology, Schulich Faculty of Chemistry, Haifa, 32000036, Israel

We explore with *ab-initio* theory high harmonic generation (HHG) from a series of gas-phase fullerenes (from C_{20} to C_{60} , including isomers) under varying laser conditions (different ellipticities, angular orientations, intensities and wavelengths). We find that HHG emission from fullerenes exhibits a prominent high-energy second plateau, extending well above the expected semi-classical cutoff, e.g. for an 800 nm driving laser with a peak intensity of $10^{14}W/cm^2$, the anomalous 2nd plateau cutoff is 115 eV. We theoretically analyze the underlying 2nd plateau physical mechanism and determine that: (i) It differs from the standard SFA-like mechanism; (ii) It is recombination-based; (iii) It has an unusual inverted cutoff scaling with wavelength (whereby the cutoff decreases with increasing wavelength, until reaching a saturation); and (iv) It exhibits a linear cutoff dependence with electric field amplitude E_0 . We further rule out real-space trajectory based pictures, indicating that the most likely culprits are sharp quantum mechanical resonances in the fullerene family. Our work establishes a new route for high energy coherent broadband emission without requiring mid-IR driving and uncovers a novel HHG mechanism in complex structure quantum systems.

Keywords: Fullerenes, C_{20} isomers, Second Plateau, Gabor Time-Frequency Analysis

High harmonic generation (HHG) is an ultrafast quantum process in which a quantum system is irradiated by an intense laser pulse and emits coherent radiation in multiples of the fundamental frequency of the driving laser[1]. This creates a broadband coherent emission that may reach up to keV range and is useful for imaging and attosecond pulse sources[2, 3], as well as for HHG-based ultrafast spectroscopy [4–15]. HHG was first explored in atoms and molecules in the gas-phase [16, 17], where it is very well understood by a mechanistic semi-classical trajectory picture for the electron dynamics [18, 19]. In this framework, the electron is (i) tunnel ionized by interaction with the laser, (ii) accelerated semi-classically in the continuum by the laser, and (iii) recombines with its parent molecule to emit an HHG photon. Over the last decade HHG has also been explored in other settings such as solids [20–30] and liquids [31–37], where somewhat similar mechanistic pictures can be obtained. However, trajectories of electrons can become much more complex in condensed media due to their numerous amount [38, 39] and weaker validity of the semi-classical picture (due to electron-electron interactions, electron-phonon interactions, etc.) [40–49]. Secondary HHG plateaus have been predicted and measured in a variety of systems and all phases of matter [21–23, 32, 50–54]. In gas-phase, it was shown that multiple plateaus can be formed due to quantum diffusion effects [52], multiple orbital contribution [51, 55, 56], or due to correlations [57]. Second plateaus are also reported recently in Rydberg atoms [53] and are known in atomic plasmas [54]. In solids and liquids, it was shown that multiple plateaus form due to long-range interactions (e.g. scattering and electron delocalization in multiple sites) [20–24, 33, 47, 52, 58, 59].

It was also predicted that a 2nd plateau should form in C_{60} and C_{70} based on tight-binding simulations that limit electron motion to the surface (i.e. in a solid-state-like setting) [50], but here the 2nd plateau energy is relatively low, up to 10 eV. Generally, all 2nd plateaus from gas/solids/liquids have not been measured or predicted in high energy ranges, mostly because their generation mechanisms relies on typical HHG mechanisms, e.g. being limited by the ionization potential or energy gap.

Fullerenes are carbon-based nanomaterials, which have drawn intensive attention in the attosecond community owing to their unique ultrafast dynamics [50, 60–67]. They are prospective candidates in a wide variety of novel fundamental and technological applications [61, 63, 68]. Earlier works have focused primarily on C_{60} , e.g. showing that HHG originates from electronic density oscillations on its surface contributed by π electrons [65], while HHG from C_{60} was measured already in 2009 with an enhanced harmonic yield compared to that of bulk carbon without appearance of a 2nd plateau [60]. However, the maximum harmonic energy reported in all of these works match typical HHG cutoffs.

Here, we perform a vast *ab-initio* study of HHG from subnanometer carbon-based fullerenes considering various laser parameters. Remarkably, we predict the existences of a wide energy 2nd plateau reaching up to 115 eV in 800 nm and $10^{14}W/cm^2$ laser conditions from all examined fullerenes (C_{20} through C_{60}). Unexpectedly, we show that the cutoff scaling law for this plateau is approximately linear with E_0 - the field amplitude, similarly to solid HHG, and exhibits a nearly linear wavelength dependence, but with a negative slope such that for longer wavelength the cutoff energy substantially decreases (until a saturation is reached). Such cutoff dependence is not known from any gas-phase, solid, or liquid systems

to date, which we believe might arise from the dual nature of fullerenes, exhibiting gas-like and solid-like features. From our vast numerical study, we uncover that: (i) the 2nd plateau is generated by a physical mechanism that differs from the 1st plateau, (ii) the mechanism is recombination-based (verified by ellipticity dependence simulations), (iii) we rule out all known trajectory-based pictures due to none providing the appropriate cutoff scaling or energy range, (iv) the effect requires a substantial excitation from the occupied orbitals to build up prior to emission. This overall leads us to conclude that the most likely culprit are strong quantum mechanical resonances. Our work sheds light on novel HHG physics in complex quantum systems and could be used for high energy coherent broadband sources that can be obtained without mid-IR drives.

Let us first describe our methodological approach. Nonlinear light-induced electron dynamics in fullerenes are studied by tracking time-evolution of the system under intense laser driving *ab-initio* with time-dependent density functional theory (TDDFT)[69]. We employ the adiabatic approximation for the exchange-correlation (XC) functional and the local density approximation, while adding a self-interaction correction (SIC) [70]. The quantum electronic dynamics follow the time-dependent Kohn-Sham (KS) equations, given as (in atomic units and length gauge)-

$$i\partial_t |\psi_j^{KS}(t)\rangle = \left[-\frac{1}{2}\Delta + \nu_{KS}(\mathbf{r}, t) - \mathbf{E}(t) \cdot \mathbf{r} \right] |\psi_j^{KS}(t)\rangle, \quad (1)$$

where the KS potential $\nu_{KS}(\mathbf{r}, t)$ can be decomposed as-

$$\nu_{KS}(\mathbf{r}, t) = V_{ion} + \int d^3r' \frac{\rho(\mathbf{r}', t)}{|\mathbf{r} - \mathbf{r}'|} + \nu_{XC}[\rho(\mathbf{r}, t)]. \quad (2)$$

Here $|\psi_j^{KS}(t)\rangle$ is the j^{th} time-dependent KS orbital. Further, V_{ion} accounts for the interaction of electrons with nuclei and core electrons, $\rho(\mathbf{r}, t)$ is the time-dependent electron density, and $\nu_{XC}[\rho(\mathbf{r}, t)]$ denotes the XC potential.

$\mathbf{E}(t)$ in equation (1) is the time-dependent electric field of the driving laser pulse. Within the dipole approximation it reads - $\mathbf{E}(t) = E_0 f(t) \cos(\omega t) \hat{x}$. E_0 is the field amplitude, $f(t)$ is the envelope function which has a \sin^2 form, and ω is the carrier frequency. Ion motion is neglected within the fixed-nuclei approximation. In order to avoid unphysical reflections of electron from the simulation box boundaries, we implement a complex absorbing potential (CAP) during the time-evolution. The induced non-linear polarization is computed from the time-dependent electron density as follows- $\mathbf{P}(t) = \int d^3r \mathbf{r} \rho(\mathbf{r}, t)$. The HHG spectrum is obtained from $\mathbf{P}(t)$ by taking Fourier transform of the dipole acceleration and filtration by the pulse envelope, and unless stated otherwise is taken as a sum of all emission polarizations.

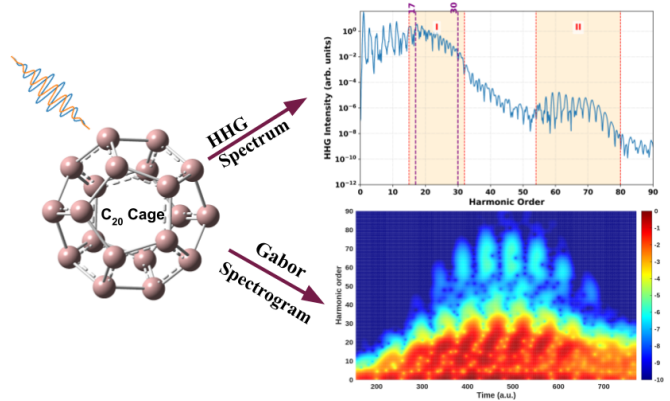


FIG. 1. (left) Illustration of set-up: C₂₀ cage irradiated by an ultrashort intense linearly polarized laser pulse, causing HHG emission. (right top panel) Exemplary HHG spectrum showing a prominent wide-energy second plateau reaching up to 115 eV. (right bottom panel) Gabor time-frequency analysis corresponding to top panel HHG spectra. The simulation is performed at 800nm driving with a peak power of 10¹⁴ W/cm².

$\rho(\mathbf{r}, t)$ is obtained by numerically solving the KS equations assuming the system is initially in the ground state (all occupied KS orbitals are propagated). All other technical details of the TDDFT simulations are delegated to the Appendix.

Within this numerical approach, we study strong laser driving of fullerenes (see Figure 1 (left) for illustration). Initially, emission is considered with a linearly polarized (along the x-axis) driving laser, with 800 nm carrier wavelength and a peak intensity of 10¹⁴ W/cm², which are standard choices for gas-phase HHG. Figure 1 (top right hand side) presents the key numerical finding: In these conditions a 2nd HHG plateau emerges at very high energies (up to 125 eV). At these energy ranges the plateau cannot be generated by the typical on-site mechanism of HHG emission from deeper orbitals (that have a higher ionization potential) - these are indicated on top of Figure 1 by dashed lines showing SFA-cutoffs [18, 19] for the HOMO and deepest occupied orbital in the system, still lacking 75 eV. Practically, this plateau is suppressed by 4 orders of magnitude from the dominant 1st plateau, which indicates a small cross section for the process behind its appearance. In order to further explore the second plateau we perform a Gabor time-frequency analysis (in Figure 1 bottom right side). The spectrum clearly shows a nearly chirp-less emission up to the 2nd plateau cutoff, which is separated from the first plateau by a wide inter-plateau decay region.

Figure 1 establishes the existence of a 2nd plateau for the smallest fullerene - C₂₀. We proceed next to search for similar signatures of secondary plateaus in all other fullerenes driven in similar conditions. Figure 2 presents calculated HHG spectra from a wide fullerene family, in-

cluding C_{20} isomers. Each panel has the same notation as shown in the Figure 1- plateaus with I/II and maximum cutoff harmonic with dashed purple lines. The second plateau proves to be a general feature of harmonic spectra from fullerenes - encompassing almost the same harmonic width, energies, and magnitudes. This universality likely partially originates from quite closely-spaced molecular orbital energies across the family, which is evident from Table I in the Appendix, though small differences still appear between systems (such as 10-20 eV shifts in cutoff energies and other features within the plateaus).

We would at this stage also note that we have performed vast convergence studies on this system (including big simulation box sizes (up to 75 a.u. box radius) and varying width of complex absorbers) in order to validate that the second plateau is a true physical feature and does not arise from numerical instabilities. These are not presented in-text, but without a doubt lead us to conclude the 2nd plateau is a meaningful feature. The coherent build-up process in the Gabor transform in Fig. 1 that follows the laser cycles also supports this conclusion. Moreover, similar effects are not observed from other small molecules such as H_2 tested in similar conditions.

We hypothesize that this high-energy emission could arise from a mixed nature of the fullerene system: On the one hand, the molecules are in the gas-phase where ionization and long trajectories are permitted as typical for HHG, while on the other hand there could still be surface dynamics of charges as arise in solids (with the surface acting like a quasi-periodic system). These effects might lead to constructive interferences with a higher energy emission. Moreover, fullerenes are well known for their resonant nature, e.g. plasmonic [61, 67, 71], which was already shown crucial in photo-ionization [61] (the first step in HHG). Therefore, it is not far-fetched to expect similar resonances leading to exponentially suppressed high energy emission windows. However, at this stage these suspicions remain to be confirmed. In what follows, we perform a broad series of simulations in order to pin-down the physical mechanism of this emission.

The first step towards this analysis is exploration of the ellipticity dependence of the harmonic spectra- whether the second plateau exists, or becomes suppressed, for higher ellipticities. Note that in typical gas-phase HHG emission yields are exponentially suppressed with the driving laser ellipticity [72], which is a tell-tale sign of an on-site recombination mechanism (with deviations from this behavior in solids [73] and liquids [32], where off-site recombination is allowed). We calculate harmonic spectra from C_{20} cage (taken as a benchmark system), driven with elliptically polarized laser pulses across all the three planes. Figure 3 shows exemplary data for two select harmonic sets- harmonics 19 and 25 from the 1st plateau, and harmonics 61 and 73 from the 2nd plateau. From Figure 3 top panels, it is evident that the 1st plateau acquires

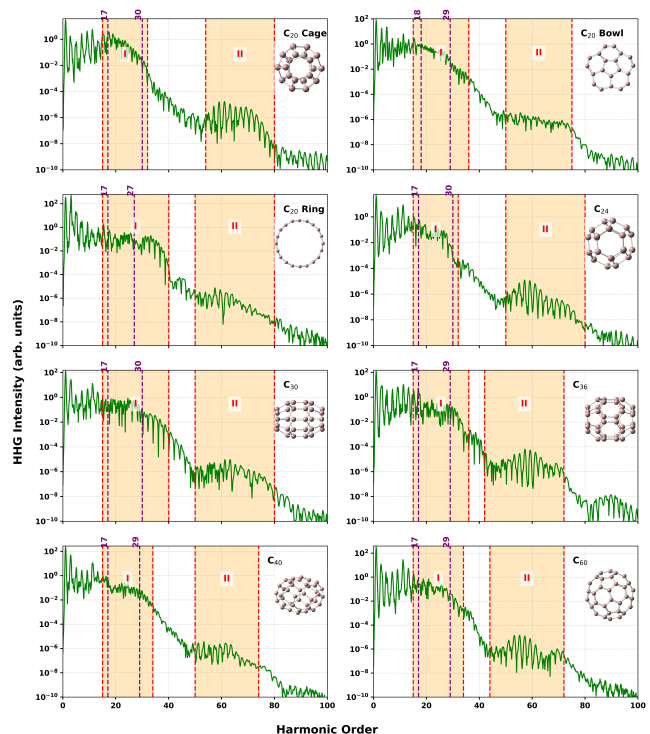


FIG. 2. HHG and 2nd plateaus from the fullerene family in similar laser conditions to Fig. 1. The geometry of each fullerene is shown in inset along with its spectrum. Plateaus are marked by background coloring, with dashed purple lines indicating typical semi-classical cutoffs from the HOMO and deepest orbital in the system.

its FWHM (of the gaussian-like decay of the harmonic signal) around an ellipticity of 0.2, which is quite typical for gas-phase HHG. On the other hand, 2nd plateau harmonics in the bottom panels reach a FWHM for an ellipticity of 0.05, which is a much narrower distribution and outlines a very fast decay with driving ellipticity. This allows us to conclude that the physical mechanism responsible for the 2nd plateau must be recombination based and on-site [74, 75] with a strict cross-section. This further rules out the possibility of an off-site recombination mechanism where recombination does not occur at the same site/center, since in such a case the ellipticity dependence widens with formation of secondary peaks [32].

After confirming an on-site recombination based mechanism for the second plateau, we proceed to explore the role of electronic correlation [57]. We consider three distinct levels of theory: (i) Full time-evolved inclusion of molecular orbitals and KS potential, labeled as full TDDFT (which is the theory level used thus-far). (ii) Restricting the KS potential to be temporally frozen to its initial form, leading to the independent particle approximation (IPA). (iii) Lastly, inclusion of the outermost HOMO orbital only leads to a single active electron ap-

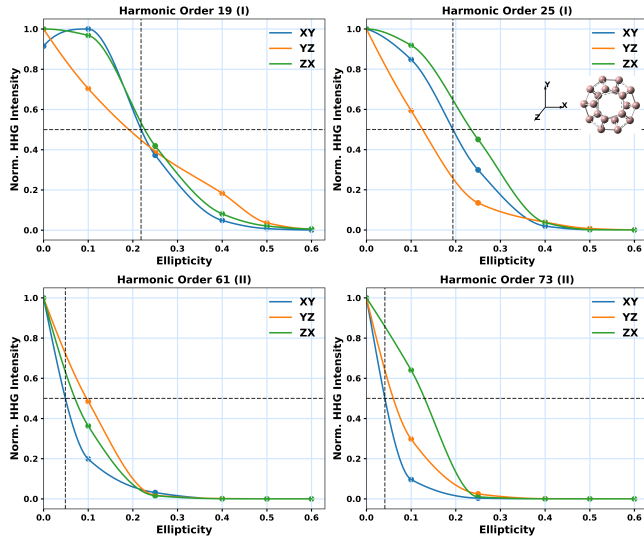


FIG. 3. Ellipticity dependence of harmonic intensity for selected harmonics from each plateau are illustrated, calculated in similar conditions to Fig. 1 but with elliptical driving. Two lines are provided as a guide to eye, passing through the full width at half maximum (FWHM) of the ellipticity-decay distribution, and its corresponding ellipticity value. 2nd plateau harmonics indicate a much sharper decay with driving ellipticity.

proximation (SAE). The results are presented in the top left panel of Fig. 4. We notice a small shift towards lower harmonics in the range of second plateau within the IPA and SAE approximations, compared to the full TDDFT case. Also, the harmonic intensity is seen slightly suppressed in the case of SAE approximation (which is expected since in this case lower lying orbitals have similar energies and also contribute). Overall though, the key observation is that electronic correlations and the multi-orbital nature of the system play a negligible role in the formation of the 2nd plateau. That is, dynamical electronic correlations are not responsible for the formation of the second plateau. We note however that non-dynamical contributions to the KS potential that include interactions between electrons are still included in all of these theory levels, which are the cause of plasmonic resonances in fullerenes; hence, these simulations do not rule out the potential role of resonances in 2nd plateau emissions.

We further investigate the harmonic spectra build-up process throughout laser sub-cycles. In the top right panel in Figure 4 we present HHG emission vs the pulse durations from 1 to 4.5 cycles, while fixing the pulse peak power. The 2nd plateau starts building up proper form for pulses longer than 1.5 cycles, with reaching the expected spectral signature at 2.5 cycle pulses. For pulses longer than 4.5 cycles no significant harmonic build-up occurs. One unique result arises - a 2nd plateau fails to emerge for pulses shorter than 1.5 cycles, even though

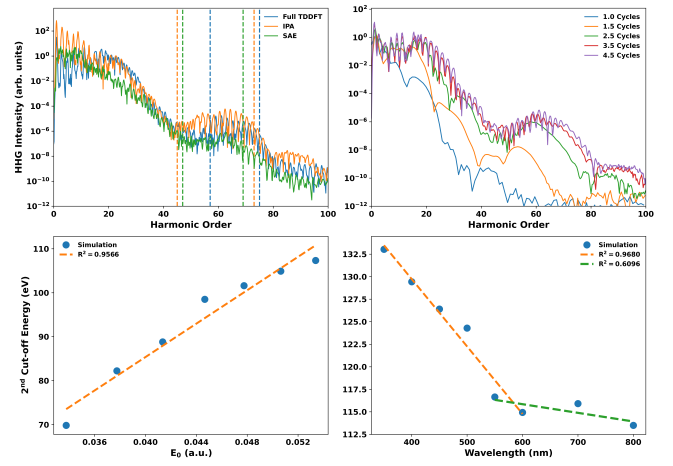


FIG. 4. Physical investigations of 2nd plateau. (Top left panel) Illustration of the negligible roles of electronic correlation and multi-orbitals contribution to the harmonic generation process in C₂₀ cage. (Top right panel) Dependence of HHG on the laser pulse duration. The second plateau regions are marked by two vertical lines. The bottom panels present cutoff scaling for the 2nd plateau with laser field strength E_0 (left) and wavelength (right). All plots calculated in similar conditions to Fig. 1 apart from the direct variations in parameters in each case.

the pulse peak power is fixed - this differs substantially from the typical SFA-like HHG mechanism [18, 19]. Indeed, in the 1st plateau one gets relatively similar emission despite shorter pulse durations, because recombining short trajectories exist, and carrier envelope phase effects play a minor role in modulating the cutoff (which can be seen in Figure 4 (top right) looking at the first plateau region that is perfectly formed for 1.5 cycle pulses). For the 2nd plateau however, the generation mechanism seems to require a build-up process. We hypothesize this could be an initial ionization process that excites a resonance for instance, or the recombination is from very long trajectories.

We perform next numerical simulations for harmonic spectra with varying laser intensities (for a fixed wavelength 800 nm) and wavelengths (for a fixed peak intensity 10^{14} W/cm^2), considering linear polarization of the driving field. Such a scan provides the cutoff law, which is usually indicative of the mechanism. Quite interestingly, our simulations (bottom panels of Figure 4) show an almost a linear dependence of the second plateau cutoff with the electric field amplitude, E_0 . Such cutoff scaling is not reported for gas-phase systems [18, 19], but is a feature common to solids [76, 77]. Coming to the cutoff scaling law for wavelength dependence, we notice a surprising feature- it shows an inverted linear dependence with the cutoff energy decreasing as the wavelength increases. This occurs until a saturation is reached around 600 nm, where the cutoff energy is roughly wavelength-independent. Such cutoff scaling has not been reported

for gas-phase systems nor for solids. In liquids, an off-site mechanism was shown to lead to a similar saturation effect, but with the exactly opposite trend for lower wavelengths, and at much lower energies (up to 20 eV) [32]. Moreover, our ellipticity-dependent results in Figure 3 clearly rule out off-site recombination. This observation unequivocally confirms that the physical origin of the second plateau differs from the SFA-type on-site recombination mechanism [18, 19]. On the basis of such unusual cutoff scaling, we expect that fullerenes showcase dual nature- exhibiting both the gas-like and solid-like features in the harmonic generation process, which somehow contributes to the 2nd plateau. The inverted wavelength dependence could also be indicative of a resonance role, since for shorter wavelengths stronger excitation to unoccupied levels and continuum states occurs, which is an important first step in resonance excitation [78–80].

We also studied the angular dependence of HHG emission from fullerenes (see Fig. 5). We noticed that the HHG yields vary differently with angles in different fullerene planes, which can have stronger/weaker dependence, depending on conditions. However, relatively similar features were also observed in the 1st plateau and are somewhat expected from the complex molecular structure. Therefore, nothing about the angular dependence seems indicative of the 2nd plateau generation process.

Typically for HHG, one expects an electronic trajectory picture to explain most basic features, certainly for cutoff scaling. This has been the case for all HHG emission explored to date (including in solids, liquids, and correlated set-ups). We attempted here to explore a similar trajectory-based picture. However, SFA-like on-site recombining trajectories inherently lack the required energies for this broad emission. Similarly, off-site recombination lacks the desired energy range, but also does not match our calculated ellipticity dependence. Coherent scattering could in principle play a role, such as scattering-assisted mechanisms. These can generally lead to much higher kinetic energies up to $10U_p$ (with U_p the ponderomotive energy). However, those still lack 50 eV energy in our conditions, and also do not match the cutoff scaling laws with field amplitude or wavelength. Conversely, we formulated a real-space trajectory model where the electron is permitted to coherently oscillate and bounce off the fullerene cage walls (inside the cage), and recombine on-site (not presented). This, however, completely fails reaching the desired energy ranges, leading to a missing 90 eV (but could still in principle contribute to 1st plateau emission). To conclude, our vast numerical and theoretical exploration strongly suggests that the fullerene 2nd plateau cannot be explained by a simple trajectory picture; rather, arises from quantum mechanical features in the system: Either surface dynamics combined with strong-field ionization, or resonances, or both. The exact origin should motivate further studies.

To summarize, we explored high harmonic generation from gas-phase fullerenes performing vast numerical *ab initio* simulations in various molecules and laser conditions. We theoretically predicted the existence of a universal second plateau in HHG from fullerenes, which emits up to 115 eV photon energies in typical HHG conditions (800 nm 10^{14} W/cm² driving laser), and has a much weaker cross-section for interaction (suppressed by 4 orders of magnitude). While we could not pinpoint the exact physical origin of this effect, our simulations unequivocally ruled out trajectory-based mechanistic pictures, established a new cutoff scaling law in this system (with inverted wavelength dependence and solid-like intensity-dependence), and showed that the emission relies on an on-site recombination mechanism that requires build-up of excitation of orbitals (not relying on correlations or multi-orbital features). This investigation hints that hidden quantum mechanical features such as resonances and surface interference could be the culprit of fullerene high-energy anomalous 2nd HHG plateaus. Our work opens new avenues for HHG physics and high-energy coherent broadband sources in complex quantum systems, and should motivate further ultrafast studies into fullerene and other caged structures.

ACKNOWLEDGMENTS

O.N. gratefully acknowledges the scientific support of Prof. Dr. Angel Rubio and the Young Faculty Award from the National Quantum Science and Technology program of Israel’s Council of Higher Education Planning and Budgeting Committee. O.N. and K.A.D. gratefully thank the Technion Helen Diller Quantum Center for financial support.

Details of TDDFT simulations

Octopus code was employed to perform all the numerical simulations [69]. We start from the ground-state (GS) calculations for the gas-phase fullerenes. The optimized geometries of the fullerenes were obtained from *ab-initio* quantum chemical calculations using gaussian [81]. The KS equations were discretized on a Cartesian grid with a spherical simulation box. The radius of the box converged at 50 a.u., which facilitates appropriate spatial dimensions for the laser-driven electronic motion and absorption. The grid spacing is taken as 0.3 a.u. in all molecules. The KS equations for the GS are solved self-consistently for each fullerene with a self-consistent field (SCF) tolerance 10^{-8} Hartree. For self-interaction correction, we choose average-density SIC that is implemented self-consistently. For the core states, we employ frozen core approximation using norm-conserving pseudopotentials [82]- LDA pseudopotentials for all our GS and time-

dependent (TD) calculations. The XC functional used throughout is the local density approximation. The calculated GS energies for HOMO and innermost orbitals for the fullerene family are provided in Table I below.

After performing the GS calculation, we carry out TDDFT simulations by propagating all occupied KS orbitals with a Lanczos propagator and a converged time step of 0.2 a.u. A complex absorbing potential is added to prevent spurious reflections of the electron from the boundaries of the simulation box with a width of 20 a.u. (converged against wider cases). For all the time-dependent simulations, the GS state is considered as the starting point (initial state). Finally, HHG spectra is computed as described in the main text by taking a Fourier transform of the dipole acceleration. The driving laser field considered is an 8-cycle long \sin^2 pulses with a peak intensity of 10^{14} W/cm² within different polarizations as discussed in the main text (with a full-width-half-maximum (FWHM) of 4 laser cycles).

Additional data

Here we present additional complementary data to the main text analysis. First, we present the KS orbital eigenenergy ranges (HOMO to deepest) in all examined systems (Table I).

TABLE I. Ionization energies for the HOMO and innermost orbitals (in a.u.) for various fullerenes.

System	HOMO	Innermost
C ₂₀ cage	-0.268971	-1.040804
C ₂₀ bowl	-0.318820	-0.957253
C ₂₀ ring	-0.250912	-0.819954
C ₂₄	-0.292205	-1.003581
C ₃₀	-0.261558	-1.006326
C ₃₆	-0.270880	-0.985806
C ₄₀	-0.278019	-0.981173
C ₆₀	-0.273401	-0.951162

Next, we present angular HHG emission data simulated by varying the linear laser polarization axis across different planes in the C₂₀ cage molecule. The data are presented for select harmonics in Fig. 5 for two harmonics from the 1st and 2nd plateaus, respectively.

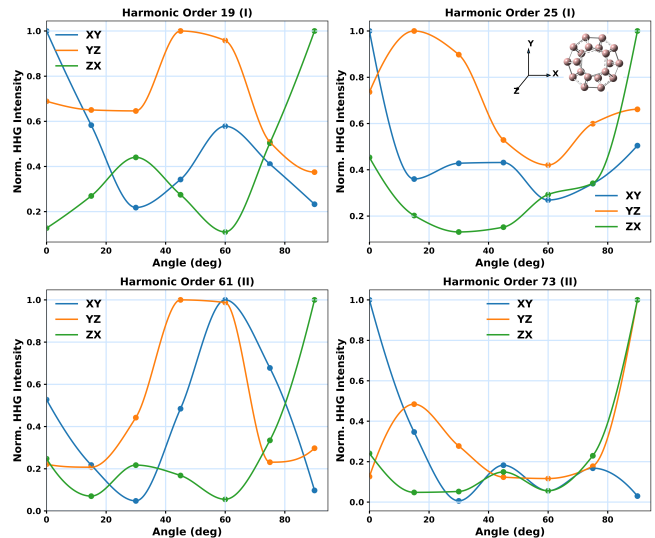


FIG. 5. Harmonic yield dependence on driving laser angle. HHG yields for select harmonics (both in the 1st and 2nd plateaus) are plotted with respect to different angular orientations of the laser electric field across all the three planes. Simulations performed in similar conditions to Fig. 1.

- [4] C. Vozzi, M. Negro, F. Calegari, G. Sansone, M. Nisoli, S. De Silvestri, and S. Stagira, *Nature Physics* **7**, 822 (2011).
- [5] J. P. Farrell, L. S. Spector, B. K. McFarland, P. H. Bucksbaum, M. Gühr, M. B. Gaarde, and K. J. Schafer, *Phys. Rev. A* **83**, 1 (2011).
- [6] R. Borrego-Varillas, M. Lucchini, and M. Nisoli, *Rep. Prog. Phys.* **85**, 066401 (2022).
- [7] O. Kneller *et al.*, *Nat. Photonics* **19**, 134 (2025).
- [8] J. P. Marangos, *J. Phys. B: At. Mol. Opt. Phys.* **49**, 132001 (2016).
- [9] S. Haessler, J. Caillat, and P. Salières, *J. Phys. B: At. Mol. Opt. Phys.* **44**, 203001 (2011).
- [10] O. Neufeld, D. Ayuso, P. Decleva, M. Y. Ivanov, O. Smirnova, and O. Cohen, *Physical Review X* **9**, 031002 (2019).
- [11] K. A. Hamer, F. Mauger, A. S. Folorunso, K. Lopata, R. R. Jones, L. F. DiMauro, K. J. Schafer, and M. B. Gaarde, *Physical Review A* **106**, 13103 (2022).
- [12] O. Neufeld and O. Cohen, *Phys. Rev. Res.* **2**, 033037 (2020).
- [13] G. Lerner, O. Neufeld, L. Hareli, G. Shoulga, E. Bordo, A. Fleischer, D. Podolsky, A. Bahabad, and O. Cohen, *Science Advances* **9**, eade0953 (2023).
- [14] D. Baykusheva and H. J. Wörner, *Phys. Rev. X* **8**, 031060 (2018).
- [15] O. Neufeld and O. Cohen, *Phys. Rev. Lett.* **123**, 103202 (2019).
- [16] M. Ferray *et al.*, *J. Phys. B: At. Mol. Opt. Phys.* **21**, L31 (1988).
- [17] V. N. Ostrovsky and J. B. Greenwood, *J. Phys. B: At. Mol. Opt. Phys.* **38**, 1867 (2005).
- [18] P. B. Corkum, *Phys. Rev. Lett.* **71**, 1994 (1993).
- [19] M. Lewenstein, P. Balcou, M. Y. Ivanov, A. L’Huillier, and P. B. Corkum, *Phys. Rev. A* **49**, 2117 (1994).
- [20] S. A. Sato *et al.*, *npj Comput. Mater.* **11**, 1 (2025).

* akankshadubey256@gmail.com

† ofern@technion.ac.il

- [1] F. Krausz and M. Ivanov, *Reviews of Modern Physics* **81**, 163 (2009).
- [2] T. Popmintchev, M.-C. Chen, P. Arpin, M. M. Murnane, and H. C. Kapteyn, *Science* **336**, 1287 (2012).
- [3] J. Gao, J. Wu, Z. Lou, F. Yang, J. Qian, Y. Peng, Y. Leng, Y. Zheng, Z. Zeng, and R. Li, *Optica* **9**, 1003 (2022).

- [21] G. Ndabashimiye *et al.*, *Nature* **534**, 520 (2016).
- [22] J.-X. Chen and X.-B. Bian, *Phys. Rev. A* **109**, 033104 (2024).
- [23] C.-M. Wang *et al.*, *Phys. Rev. Res.* **2**, 033333 (2020).
- [24] S. Ghimire, A. D. DiChiara, E. Sistrunk, P. Agostini, L. F. DiMauro, and D. A. Reis, *Nature Physics* **7**, 138 (2011).
- [25] C. S. Hansen *et al.*, *Commun. Chem.* **5**, 94 (2022).
- [26] H. Kim, J. Kim, A. Galler, M. Kim, A. Chacón, K. Watanabe, T. Taniguchi, D. Kim, S. Chae, M.-H. Jo, A. Rubio, O. Neufeld, and J.-W. Kim, *Nature Communications* **16**, 9825 (2025).
- [27] A. Uzan-Narovlansky, A. Jimenez-Galan, G. Orenstein, R. Silva, T. Arusi-Parpar, S. Shames, B. Bruner, B. Yan, O. Smirnova, M. M. Ivanov, and N. Dudovich, *Nature Photonics* **16**, 428 (2022).
- [28] M. Hohenleutner, F. Langer, O. Schubert, M. Knorr, U. Huttner, S. W. Koch, M. Kira, and R. Huber, *Nature* **523** (2015).
- [29] O. Neufeld, N. Tancogne-Dejean, H. Hübener, U. De Giovannini, and A. Rubio, *Phys. Rev. X* **13**, 031011 (2023).
- [30] L. Yue and M. B. Gaarde, *Phys. Rev. Lett.* **124**, 153204 (2020).
- [31] A. Mondal, B. Waser, T. Balciunas, O. Neufeld, Z. Yin, N. Tancogne-Dejean, A. Rubio, and H. J. Wörner, *Optics Express* **31**, 34348 (2023).
- [32] A. Mondal *et al.*, *Nat. Photonics* 10.1038/s41566-025-01805-y (2025).
- [33] T. T. Luu, Z. Yin, A. Jain, *et al.*, *Nat. Commun.* **9**, 3723 (2018).
- [34] S. Mondal, O. Neufeld, X. Yin, Z. Nourbakhsh, V. Svoboda, A. Rubio, N. Tancogne-Dejean, and H. J. Wörner, *Nature Physics* **19**, 1813 (2023).
- [35] O. Neufeld, Z. Nourbakhsh, N. Tancogne-Dejean, and A. Rubio, *Journal of Chemical Theory and Computation* **18**, 4117 (2022).
- [36] A.-W. Zeng and X.-B. Bian, *Phys. Rev. Lett.* **124**, 203901 (2020).
- [37] E. Moore, S. Giri, A. Koutsogiannis, T. Alavi, G. McCracken, K. Lopata, J. M. Herbert, M. B. Gaarde, and L. F. DiMauro, *Proceedings of the National Academy of Sciences* **122**, e2514825122 (2025).
- [38] L. Yue and M. B. Gaarde, *J. Opt. Soc. Am. B* **39**, 535 (2022).
- [39] S. Ghimire and D. A. Reis, *Nature Physics* **15**, 10 (2019).
- [40] K. Uchida, G. Mattoni, S. Yonezawa, F. Nakamura, Y. Maeno, and K. Tanaka, *Physical Review Letters* **128**, 127401 (2022).
- [41] N. Tancogne-Dejean, F. G. Eich, and A. Rubio, *npj Computational Materials* **8**, 145 (2022).
- [42] J. Freudenstein, M. Borsch, M. Meierhofer, D. Afanasiev, C. P. Schmid, F. Sandner, M. Liebich, A. Girnghuber, M. Knorr, M. Kira, and R. Huber, *Nature* **610**, 290 (2022).
- [43] V. Chang Lee, L. Yue, M. B. Gaarde, Y.-h. Chan, and D. Y. Qiu, *Nature Communications* **15**, 6228 (2024).
- [44] D. Freeman, A. Kheifets, S. Yamada, A. Yamada, and K. Yabana, *Physical Review B* **106**, 75202 (2022).
- [45] S. V. B. Jensen, L. B. Madsen, A. Rubio, and N. Tancogne-Dejean, *Physical Review A* **109**, 63104 (2024).
- [46] O. Neufeld, Y. Zhang, U. De Giovannini, H. Hübener, and A. Rubio, *Proc. Natl. Acad. Sci. U.S.A.* **119**, e2204219119 (2022).
- [47] J. Zhang, Z. Wang, F. Lengers, D. Wigger, D. E. Reiter, T. Kuhn, H. J. Wörner, and T. T. Luu, *Nature Photonics* **18**, 792 (2024).
- [48] N. Tancogne-Dejean, M. A. Sentef, and A. Rubio, *Phys. Rev. Lett.* **121**, 097402 (2018).
- [49] N. Rana and G. Dixit, *Phys. Rev. A* **106**, 053116 (2022).
- [50] H. K. Avetissian, A. G. Ghazaryan, and G. F. Mkrtchian, *Phys. Rev. B* **104**, 125436 (2021).
- [51] E. Luppi and E. Coccia, *The Journal of Physical Chemistry A* **127**, 7335 (2023).
- [52] Z. Tang *et al.*, *Opt. Express* **33**, 30634 (2025).
- [53] N.-L. Phan *et al.*, *J. Opt. Soc. Am. B* **37**, 1781 (2020).
- [54] R. A. Ganeev, *Opt. Spectrosc.* **105**, 930 (2008).
- [55] X. Xie *et al.*, *Chin. Phys. Lett.* **42**, 100301 (2025).
- [56] O. Neufeld, N. Tancogne-Dejean, and A. Rubio, *The Journal of Physical Chemistry Letters* **15**, 7254 (2024).
- [57] A. de las Heras, C. Hernández-García, and L. Plaja, *Phys. Rev. Res.* **2**, 033047 (2020).
- [58] A. J. Uzan-Narovlansky *et al.*, *Nat. Photonics* **16**, 428 (2022).
- [59] A. J. Uzan, G. Orenstein, Á. Jiménez-Galán, M. B. Gaarde, M. Y. Ivanov, and N. Dudovich, *Nature Photonics* **14**, 183 (2020).
- [60] R. A. Ganeev, L. B. E. Bom, J. Abdul-Hadi, M. C. H. Wong, J. P. Brichta, V. R. Bhardwaj, and T. Ozaki, *Phys. Rev. Lett.* **102**, 013903 (2009).
- [61] S. Biswas *et al.*, *Sci. Adv.* **11**, eads0494 (2025).
- [62] T. Barillot *et al.*, *Phys. Rev. A* **91**, 033413 (2015).
- [63] E. Ali *et al.*, *J. Phys. Chem. A* **129**, 2123 (2025).
- [64] T. Topcu, E. A. Bleda, and Z. Altun, *Phys. Rev. A* **100**, 063421 (2019).
- [65] A. P. Woźniak and R. Moszyński, *J. Phys. Chem. A* **128**, 2683 (2024).
- [66] G. P. Zhang and Y. H. Bai, *Phys. Rev. B* **101**, 081412(R) (2020).
- [67] P. V. Redkin, M. B. Danailov, and R. A. Ganeev, *Phys. Rev. A* **84**, 013407 (2011).
- [68] Q. Xu, D. Weinberg, M. S. Okyay, M. Choi, M. Del Ben, and B. M. Wong, *Journal of the American Chemical Society* **146**, 35313 (2024).
- [69] N. Tancogne-Dejean *et al.*, *Journal of Chemical Physics* **152**, 124119 (2020).
- [70] C. Legrand, E. Suraud, and P.-G. Reinhard, *J. Phys. B* **35**, 1115 (2002).
- [71] N. L. Matsko and I. A. Kruglov, *The Journal of Physical Chemistry Letters* **12**, 11873 (2021).
- [72] M. Möller, Y. Cheng, S. D. Khan, B. Zhao, K. Zhao, M. Chini, G. G. Paulus, and Z. Chang, *Phys. Rev. A* **86**, 011401 (2012).
- [73] L. Yue and M. B. Gaarde, *J. Opt. Soc. Am. B* **39**, 535 (2022).
- [74] T. Kanai, S. Minemoto, and H. Sakai, *Phys. Rev. Lett.* **98**, 053002 (2007).
- [75] K. S. Budil *et al.*, *Phys. Rev. A* **48**, R3437 (1993).
- [76] G. Vampa, C. R. McDonald, G. Orlando, D. D. Klug, P. B. Corkum, and T. Brabec, *Phys. Rev. Lett.* **113**, 073901 (2014).
- [77] X. Liu, X. Zhu, X. Zhang, D. Wang, P. Lan, and P. Lu, *Optics Express* **25**, 29216 (2017).
- [78] V. Strelkov, *Phys. Rev. Lett.* **104**, 123901 (2010).
- [79] M. Tudorovskaya and M. Lein, *Physical Review A* **84**, 013430 (2011).
- [80] Y. Aharon, A. Pick, A. Hen, G. Marcus, and O. Neufeld,

- Phys. Rev. Res. **8**, 013063 (2026).
- [81] M. J. Frisch, G. W. Trucks, H. B. Schlegel, G. E. Scuseria, M. A. Robb, J. R. Cheeseman, G. Scalmani, V. Barone, G. A. Petersson, H. Nakatsuji, X. Li, M. Caricato, A. V. Marenich, J. Bloino, B. G. Janesko, R. Gomperts, B. Mennucci, H. P. Hratchian, J. V. Ortiz, A. F. Izmaylov, J. L. Sonnenberg, D. Williams-Young, F. Ding, F. Lipparini, F. Egidi, J. Goings, B. Peng, A. Petrone, T. Henderson, D. Ranasinghe, V. G. Zakrzewski, J. Gao, N. Rega, G. Zheng, W. Liang, M. Hada, M. Ehara, K. Toyota, R. Fukuda, J. Hasegawa, M. Ishida, T. Nakajima, Y. Honda, O. Kitao, H. Nakai, T. Vreven, K. Throssell, J. A. Montgomery, Jr., J. E. Peralta, F. Ogliaro, M. J. Bearpark, J. J. Heyd, E. N. Brothers, K. N. Kudin, V. N. Staroverov, T. A. Keith, R. Kobayashi, J. Normand, K. Raghavachari, A. P. Rendell, J. C. Burant, S. S. Iyengar, J. Tomasi, M. Cossi, J. M. Millam, M. Klene, C. Adamo, R. Cammi, J. W. Ochterski, R. L. Martin, K. Morokuma, O. Farkas, J. B. Foresman, and D. J. Fox, Gaussian~16 Revision C.01 (2016), gaussian Inc. Wallingford CT.
- [82] C. Hartwigsen, S. Goedecker, and J. Hutter, Phys. Rev. B **58**, 3641 (1998).